AL-Bahir
Journal for Engineering and Pure Sciences
BJEPS

Volume 5 | Issue 2 Article 1

Analysis of the effect of vaccination, efficient surveillance and treatment on the transmission dynamics of cholera

Loyinmi Adedapo Chris
Department of Mathematics Tai Solarin University of Education, Ijagun, Ijebu Ode, Ogun State. Nigeria.

Ajala Adebisi Shukurat
Department of Mathematics, Tai Solarin University of Education, Ijagun, Ijebu Ode. Ogun State. Nigeria

Alani L. Ijaola
Department of Mathematics, Federal University of Agriculture, Abeokuta, Ogun State. Nigeria.

Recommended Citation

Chris, Loyinmi Adedapo; Shukurat, Ajala Adebisi; and Ijaola, Alani L. (2024) "Analysis of the effect of vaccination, efficient surveillance and treatment on the transmission dynamics of cholera," *Al-Bahir*: Vol. 5: Iss. 2, Article 1.
Available at: https://doi.org/10.55810/2313-0083.1070

Analysis of the effect of vaccination, efficient surveillance and treatment on the transmission dynamics of cholera

Source of Funding

The authors declare that no funds, grants, or other support were received to prepare this manuscript

Conflict of Interest

The authors declare that they have no competing interests

Data Availability

No datasets were generated or analyzed during the current study.

Author Contributions

Authors contributed equally

ORIGINAL STUDY

Analysis of the Effect of Vaccination, Efficient Surveillance and Treatment on the Transmission Dynamics of Cholera

Adedapo C. Loyinmi [a,*], Adebisi S. Ajala [a], Ijaola L. Alani [b]

[a] Department of Mathematics, Tai Solarin University of Education, Ijagun, Ijebu Ode, Ogun State, Nigeria
[b] Department of Mathematics, Federal University of Agriculture, Abeokuta, Ogun State, Nigeria

Abstract

In this study, we presented a modified SIR-SI model to investigate the dynamics and potential controls for cholera transmission, with an incident rate equipped with a saturation factor to investigate the combined impact of three vital measures which include effective surveillance, vaccination campaign and proper treatment in case severity. We established among other things, the qualitative analysis of the model to validate the results. Furthermore, the reproduction number (R_0) was found to be less than unity (1), through the stability analysis. Additionally, finite different scheme was utilized in solving the differential equations of the model. MATLAB software was used for the numerical simulation to examine the effect of these control measures on the population density, findings from the graphical solutions depicts that these measures will aid in flattening the curve Cholera propagation in the population if properly implemented.

Keywords: Cholera, Stability, Endemic, Control strategies, Optimal control

1. Introduction

The impact of common calamities including extreme weather, wildfires, earthquakes, heavy rains, and floods is significant for the human population. Aside from these, the global spread of infectious diseases is one of the most significant problems facing humanity. Numerous people get crippled as a result of these diseases, and the cost of treating human health concerns is high [1–3]. The bacteria *Vibrio cholerae* is the cause of cholera, a watery diarrheal illness. The usage of contaminated food, particularly fish, and water are the primary and most fundamental causes of the cholera epidemic [4–8]. The transmission of cholera can occur through direct contact between humans as well as indirect human-to-environment contact. Household individuals who are cholera patients are particularly vulnerable to infection, potentially as a result of contaminated household water storage containers or contaminated food preparation [3–11]. A small number of places in North America and Europe, as well as South Africa, are home to the majority of cholera cases [12]. Asia has been the source of seven cholera pandemics that have struck humanity since 1817. The seventh cholera pandemic started in 1961 in Indonesia and lasted over forty years, making it the longest outbreak in recorded history [13–15]. The first signs of cholera in patients are loose, watery stools. Dehydration, a reduction in blood pressure, and renal failure may result from these. If treatment is delayed, death might occur in a matter of days. In recent times, there have been several cholera outbreaks in South Asia, Africa, and South America. The World Health Organization (WHO) estimates that 3–5 million cases of illness occur each year in these regions [16–18]. Any infectious disease's mechanism can be understood with the use of mathematical modelling. We can gain a profound understanding of disease transmission with the help of the relevant

Received 21 June 2024; revised 16 July 2024; accepted 20 July 2024.
Available online 16 August 2024

* Corresponding author.
E-mail addresses: loyinmiac@tasued.edu.ng (A.C. Loyinmi), adebisiajala17@gmail.com (A.S. Ajala), ijaolaal@funaab.edu.ng (I.L. Alani).

https://doi.org/10.55810/2313-0083.1070

theoretical framework. It also aids in the accurate and effective planning of our infection control approach. The SIR model, which divides the population into three compartments—susceptible, infectious, and recovered—is the fundamental model used to describe the spread of infectious diseases. In 1929, Kermack and McKendrick put out this model [19]. For a deeper understanding, a plethora of mathematical models based on the system of ordinary differential equations have been presented for cholera infection. The cholera model was created in 1979 by Capasso and Paveri-Fontana and consisted of two ordinary differential equations: the population of bacteria and the population of infected humans. They conducted phase space analysis and came to the conclusion of their results [20–22]. They also established the minimal requirements for the spread of endemic and epidemic cholera. A structure based on hierarchies has been utilized to describe the influence on natural factors, such as meteorological or climate-related variables, in Refs. [23–25]. Jensen and colleagues examined the function of bacteriophages in managing cholera outbreaks. Patients suffering from cholera are split into two groups: those infected with *V. cholerae* only and those infected with both *V. cholerae* and phage. They discovered that bacteriophage induction can lessen the intensity of a cholera outbreak and aid in its decline [26–30]. Longini et al. talked about using oral vaccine (rehydration treatment) to manage prevalent cholera [31–33]. Three interventions were introduced by Neilan et al. to construct the optimum control problem: rehydrating and treating cholera patients with antibiotics; immunizing vulnerable individuals; and maintaining water sanitation. For both asymptomatic and symptomatic people, the effectiveness of single and combination controls has been visually displayed in Refs. [34–37]. The cholera disease model was qualitatively analyzed in 2011 by Mwasa et al., both with and without public health interventions. These interventions consist of immunization drives, educational campaigns, and the care of contagious people. They identified the prerequisites for reducing the fundamental reproduction number that is brought about by education, immunization, and therapy [38–42]. In 2017, Lemo-Paiáo et al. investigated the model of cholera disease propagation by assuming that treatment control was carried out on isolated patients. In this investigation, the assumption of contaminated person isolation has been made [43,44] (see Fig. 1).

Many studies on Cholera propagation abound but the present ravaging manner by which Cholera springs up unexpectedly around the globe despite existing measures implies continuous study on

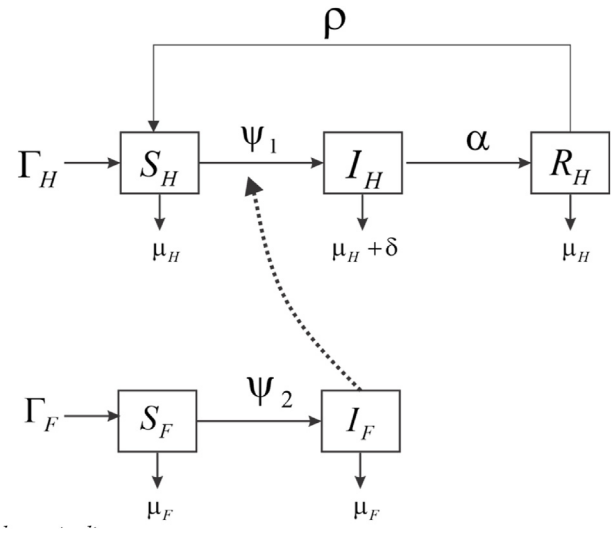

Fig. 1. Cholera schematic diagram.

taming this killer infection cannot be over emphasized. Many part of the globe still don't have access to quality drinkable water and sanitized environment, hence we hereby further investigate the effects of measures and combination of measures on the transmission dynamics of this deadly infection with a modified SIR-SI epidemic model between host and vector, solving the system of equations numerically using finite difference element method.

2. Model description

The current model for cholera transmission is based on the division of the entire population, represented by the variable (N), into two distinct groups: (N_h) for humans and (N_f) for flies. This division allows us to study the dynamics of the disease separately within these two major groups.

In this model, (N_h) represents the human population, which includes individuals susceptible to cholera, those who have been infected and recovered human (S_h, I_h, R_h). On the other hand, N_f represents the flies' population. Additionally, the rates at which flies and humans are recruited into the system through immigration or birth are Γ_H and Γ_F, respectively as the rate of transmission of the cholera bacterium to humans and flies is Ψ_1 to Ψ_2, respectively, when they come into contact with an infected person's stools.

$$\Psi_1 = \frac{\beta_1 I_H}{1+\Phi I_H} + \frac{\beta_2 I_F}{1+\Phi I_F} \tag{1}$$

$$\Psi_2 = \frac{\beta_3 I_F}{1+\Phi I_F} \tag{2}$$

3. The cholera model

In order to describe the dynamics of the bacterium, the following system of ordinary differential equations has been developed, based on the detailed description and basic assumptions of the model:

$$\left.\begin{aligned}\frac{dS_H}{dt} &= \Gamma_H + \rho R_H - (\Psi_1 + \mu_H)S_H \\ \frac{dI_H}{dt} &= \Psi_1 S_H - (\alpha + \mu_H + \delta)I_H \\ \frac{dR_H}{dt} &= \alpha I_H - (\rho + \mu_H)R_H\end{aligned}\right\} \tag{3}$$

$$\left.\begin{aligned}\frac{dS_F}{dt} &= \Gamma_F - (\Psi_2 + \mu_F)S_F \\ \frac{dI_H}{dt} &= \Psi_2 S_F - \mu_F I_F\end{aligned}\right\} \tag{4}$$

3.1. Mathematical analyzing the cholera model

3.1.1. Existence and uniqueness of solution

Using the Lipschitz condition, from the systems of equations (3) and (4)

$$\begin{aligned}G_1 &= \Gamma_H + \rho R_H - (\psi_1 + \mu_H)S_H \\ G_2 &= \psi_1 S_H - (\alpha + \mu_H + \delta)I_H \\ G_3 &= \alpha I_H - (\rho + \mu_H)R_H \\ G_4 &= \Gamma_F - (\psi_2 + \mu_F)S_F \\ G_5 &= \psi_2 S_F - \mu_F I_F\end{aligned} \tag{5}$$

Theorem 1. Let K denote the region $0 \le \chi \le M$, then the systems of equation (5) possess a unique solution if and only if $\frac{\partial G_i}{\partial b_j}$ are continuous and bounded in K, for $i \neq j$

Proof

We need to establish the partial derivative (5) with respect to the state variables which yield;

$$\left|\frac{\partial G_1}{\partial S_H}\right| = |-(\Psi_1 + \mu_H)| < \infty, \left|\frac{\partial G_1}{\partial I_H}\right| = |0| < \infty, \left|\frac{\partial G_1}{\partial R_H}\right| = |\rho| < \infty,$$

$$\left|\frac{\partial G_2}{\partial S_H}\right| = |\Psi_1| < \infty, \left|\frac{\partial G_2}{\partial I_H}\right| = |-(\alpha + \mu_H + \delta)| < \infty, \left|\frac{\partial G_2}{\partial R_H}\right| = |0| < \infty,$$

$$\left|\frac{\partial G_3}{\partial S_H}\right| = |0| < \infty, \left|\frac{\partial G_3}{\partial I_H}\right| = |\alpha| < \infty, \left|\frac{\partial G_3}{\partial R_H}\right| = |-(\rho + \mu_H)| < \infty,$$

$$\left|\frac{\partial G_4}{\partial S_F}\right| = |-(\Psi_2 + \mu_F)| < \infty, \left|\frac{\partial G_4}{\partial I_F}\right| = |0| < \infty,$$

$$\left|\frac{\partial G_5}{\partial S_F}\right| = |\Psi_2| < \infty, \left|\frac{\partial G_5}{\partial I_F}\right| = |-\mu_F| < \infty$$

Clearly from the partial derivative above of system (5), the solutions to the systems of equations exist, unique and remains bounded.

3.1.2. Positivity and boundedness of the solution

In this section, we demonstrate that the variables representing population compartments maintain non-negative throughout the simulation. Additionally, we establish that the total population remains constant at all time. This implies that from the human population N_H=$S_H + I_H + R_H$ is written as;

$$\frac{dN_H}{dt} = \frac{dS_H}{dt} + \frac{dI_H}{dt} + \frac{dR_H}{dt}$$

And putting in each state variable accordingly we obtain

$$\frac{dN_H}{dt} = \Gamma_H - \mu_F N_H - \delta_H(I_H) \tag{6}$$

Furthermore, for the reservoir's system, where (4) and the corresponding differential equations are given as follows:

$$\frac{dN_F}{dt} = \Gamma_F - \mu_F N_F \tag{7}$$

Theorem 2. Let $(S_H, I_H, R_H, S_F, I_F)$be the solution of the cholera system equation (3) and (4) with the initial conditions in a feasible region $\Pi = \Pi_H \times \Pi_F$ where:

$$\Pi_H = (S_H, I_H, R_H) \in R_+^3 : N_H \le \frac{\Gamma_H}{\mu_H} \tag{8}$$

And

$$\Pi_H = (S_F, I_F) \in R_+^2 : N_F \leq \frac{\Gamma_F}{\mu_F} \tag{9}$$

Then Π is positive invariant.

Solving (6), with the method of integrating factor, we have

$$\frac{dN_H}{dt} = \Gamma_H - \mu_H N_H$$

Where $\delta_F = 0$ at DFE

$$\text{As } t \to \infty, N_H(t) \leq \frac{\Gamma_H}{\mu_H} \tag{10}$$

Similarly, by applying the use of integrating on (7), we obtain:

$$\frac{dN_F}{dt} = \Gamma_F - \mu_F N_F$$

$$\text{As } t \to \infty\, N_H(t) \leq \frac{\Gamma_H}{\mu_H} \tag{11}$$

Here, we are able to establish that the model is well posed mathematically for time (t).

3.2. Presence of the cholera-free equilibrium state

The term "cholera-free equilibrium state" describes a stable situation in which the population under consideration is resistant to the illness.

Thus $S_H^0 \neq 0,\ S_F^0 \neq 0$

For $S_H^0 \neq 0, I_H^0 = 0, R_H^0 = 0,$ and $S_F^0 \neq 0, S_F^0 = 0,$

Then, the systems (10) and (11) become

$$\Gamma_H - \mu_H S_H^0 = 0$$
$$\Gamma_F - \mu_F S_F^0 = 0$$

Thus gives

$$S_H^0 = \frac{\Gamma_H}{\mu_H}$$

$$S_F^0 = \frac{\Gamma_F}{\mu_F} \tag{12}$$

This gives us the DFE point for the human and the flies' population,

$E^0 = (S_H^0, I_H^0, R_H^0, S_F^0, I_F^0,) = \left(\frac{\Gamma_H}{\mu_H}, 0, 0, \frac{\Gamma_F}{\mu_F}, 0\right)$ is the DFE points for the proposed system.

3.3. Basic reproduction number

The basic reproduction number of the cholera bacteria, was denoted as *Rn* is a critical epidemiological parameter that signifies the potential for the disease to spread in a population without any immunity.

Mathematically, the basic reproduction number *Rn* was calculated based on the parameters of the disease transmission and progression. This basic reproduction number *Rn* provides valuable information about the potential severity and speed of an outbreak. The accurate estimation of this our *Rn* is crucial for public health officials to understand the dynamics of an outbreak and design effective control measures to prevent and contain the spread of the cholera bacteria. From the system of ODEs, equation (3) and (4). And by utilizing the next generation matrix method.

To calculate the reproduction number, we only consider the terms related to infected compartments.

$$R_n = \Delta\left(FV^{-1}\right) \tag{13}$$

Where F is the matrix of new infection and V is the matrix of other transfer terms infection Δ is the spectral radius of FV^{-1}

$$F = \begin{bmatrix} \Psi_1 S_H \\ \Psi_2 S_F \\ 0 \\ 0 \\ 0 \end{bmatrix}, V = \begin{bmatrix} (\alpha + \mu_H + \delta) I_H \\ \mu_F \\ -\Gamma_H - \rho R_H + (\psi_1 + \mu_H) S_H \\ -\Gamma_F + (\psi_2 + \mu_F) S_F \\ -\alpha I_H + (\rho + \mu_H) R_H \end{bmatrix} \tag{14}$$

Solving 14 using (13)

The spectral radius for both human and fly population is;

$$R_{0H} = \frac{\beta_1 S_H}{(\alpha + \mu_H + \delta)(1 + \Phi I_H)^2}, R_{0F} = \frac{\beta_3 S_F}{\mu_F (1 + \Phi I_F)^2}$$

$$R_n = \sqrt{R_{0H} R_{0F}}$$

$$R_n = \sqrt{\frac{\beta_1\beta_2\beta_3\Gamma_H\Gamma_F}{\mu_F^2\mu_H(\alpha+\mu_H+\delta)(1+\Phi I_H)^2(1+\Phi I_F)^2}} \tag{15}$$

3.4. Stability analysis

3.4.1. Local stability

Theorem 3. If $R_0 < 1$, then the system (3, 4) is locally asymptotically stable (LAS), and unstable otherwise

Proof
We establish the above theorem by calculating the Jacobian matrix of system in (3, 4) at DFE point

$$E^0 = (S_H^0, I_H^0, R_H^0, S_F^0, I_F^0,) = \left(\frac{\Gamma_H}{\mu_H}, 0, 0, \frac{\Gamma_F}{\mu_F}, 0\right)$$

It is necessary for the computation of the stability $J(S_H, I_H, R_H, S_F, I_F)$ of the system which is given as;

$$J = \begin{bmatrix} -\mu_H & \frac{\beta_1\Gamma_H}{\mu_H} & \rho & 0 & -\frac{\beta_2\Gamma_H}{\mu_H} \\ 0 & \frac{\beta_1\Gamma_H}{\mu_H} - (\alpha+\mu_H+\delta) & 0 & 0 & \frac{\beta_2\Gamma_H}{\mu_H} \\ 0 & \alpha & -(\rho+\mu_H) & 0 & 0 \\ 0 & 0 & 0 & -\mu_F & \frac{\beta_3\Gamma_F}{\mu_F} \\ 0 & 0 & 0 & 0 & \frac{\beta_3\Gamma_F}{\mu_F} - \mu_F \end{bmatrix} \tag{16}$$

Now, the eigenvalue yields:

$$|J-\lambda I| = \begin{bmatrix} -\mu_H-\lambda & \frac{\beta_1\Gamma_H}{\mu_H} & \rho & 0 & -\frac{\beta_2\Gamma_H}{\mu_H} \\ 0 & \frac{\beta_1\Gamma_H}{\mu_H} - (\alpha+\mu_H+\delta) - \lambda & 0 & 0 & \frac{\beta_2\Gamma_H}{\mu_H} \\ 0 & \alpha & -(\rho+\mu_H)-\lambda & 0 & 0 \\ 0 & 0 & 0 & -\mu_F-\lambda & \frac{\beta_3\Gamma_F}{\mu_F} \\ 0 & 0 & 0 & 0 & \frac{\beta_3\Gamma_F}{\mu_F} - \mu_F - \lambda \end{bmatrix} \tag{17}$$

Now at DFE

After necessary simplification on (17), we obtain the Eigen Values as;

$$\lambda_1 = -\mu_H, \lambda_2 = -(\mu_H+\rho),$$
$$\lambda_3 = -\left((\alpha+\mu_H+\delta) - \frac{\beta_1\Gamma_H}{\mu_H}\right), \lambda_4 = -\mu_F, \lambda_5 = \mu_H,$$
$$\lambda_5 = -\mu_F + \frac{\beta_3\Gamma_F}{\mu_F}$$

From $\lambda_3 = -\left((\alpha+\mu_H+\delta) - \frac{\beta_1\Gamma_H}{\mu_H}\right)$ and $\lambda_5 = -\mu_F + \frac{\beta_3\Gamma_F}{\mu_F}$

$$R_{0H} = \frac{\beta_1 S_H}{(\alpha+\mu_H+\delta)(1+\Phi I_H)^2}\ R_{0F} = \frac{\beta_3 S_F}{\mu_F(1+\Phi I_F)^2}$$

$$\lambda_3 = -\left((\alpha+\mu_H+\delta) - \frac{\beta_1\Gamma_H}{\mu_H}\right)$$

From λ_3 we can write that

$$\lambda_3 = -(\alpha+\mu_H+\delta)\left(1 - \frac{\beta_1 S_H}{(\alpha+\mu_H+\delta)(1+\Phi I_H)^2}\right)$$

$$\lambda_3 = -(\alpha+\mu_H+\delta)\left(1-\frac{\beta_1 S_H}{(\alpha+\mu_H+\delta)(1+\Phi I_H)^2}\right) \leq -(\alpha+\mu_H+\delta)(1-R_{0H}) \tag{18}$$

And

$$\lambda_5 = -\mu_F\left(1-\frac{\beta_3 S_F}{\mu_F(1+\Phi I_F)^2}\right)$$

$$\lambda_5 = -\mu_F\left(1-\frac{\beta_3 S_F}{\mu_F(1+\Phi I_F)^2}\right) \leq -\mu_F(1-R_{0F}) \tag{19}$$

Since (18) and (19) remain negative (stable) then R_{0H} <1 and R_{0F} <1. Hence Theorem 2 has been established.

3.5. Global stability of disease-free equilibrium (DFE) Theorem 4

The positive equilibrium point of system (3, 4) is globally stable, if $R_0 < 1$.

Proof

Using the method of Lyapunov function to establish stability at E^0, the following Lyapunov function was constructed.

$$G(S_H,I_H,R_H,S_F,I_F) = \left(S_H - S_H^0 - S_H^0\log\frac{S_H^0}{S_H}\right) + \left(I_H - I_H^0 - I_H^0\log\frac{I_H^0}{I_H}\right) + \left(R_H - R_H^0 - R_H^0\log\frac{R_H^0}{R_H}\right) + \left(S_F - S_F^0 - S_F^0\log\frac{S_F^0}{S_F}\right) + \left(I_F - I_F^0 - I_F^0\log\frac{I_F^0}{I_F}\right) \tag{20}$$

By direct calculation and solving for the derivative of G along the system path of (3, 4) we obtain;

$$\frac{dK}{dt} = \left(\frac{S_H-S_H^0}{S_H}\right)\frac{dS_H}{dt} + \left(\frac{I_H-I_H^0}{I_H}\right)\frac{dI_H}{dt} + \left(\frac{R_H-R_H^0}{R_H}\right)\frac{dR_H}{dt} + \left(\frac{S_F-S_F^0}{S_F}\right)\frac{dS_F}{dt} + \left(\frac{I_F-I_F^0}{I_F}\right)\frac{dI_F}{dt} \tag{21}$$

Expanding (21), representing the positive and negative terms with X and Y respectively, we have;

$$\frac{dK}{dt} = X - Y$$

$$P = \left(1-\frac{S_H^0}{S_H}\right)(\Gamma_H+\rho R_H) + \left(1-\frac{I_H^0}{I_H}\right)\Psi_1 S_H + \left(1-\frac{R_H^0}{R_H}\right)\alpha I_H + \left(1-\frac{S_F^0}{I_F}\right)\Gamma_F + \left(1-\frac{I_F^0}{I_F}\right)\Psi_2 S_F \tag{22}$$

Similarly,

$$N = \frac{(S_H-S_H^0)^2}{S_H}(\Psi_1+\mu_H) + \frac{(1_H-1_H^0)^2}{I_H}(\alpha+\mu_H+\delta) + \frac{(R_H-R_H^0)^2}{R_H}(\rho+\mu_H) + \frac{(S_F-S_F^0)^2}{S_F}(\Psi_2+\mu_F) + \frac{(I_F-I_F^0)^2}{I_F}\mu_F \tag{23}$$

If $X<Y$, then $\frac{dK}{dt}$ will be negative definite along the system (solution) path. And so, means only at Cholera bacteria free system (E^0) would $\frac{dK}{dt} \leq 0$. This simply means the system is stable globally at the Cholera bacteria disease free system.

3.6. Existence of the endemic equilibrium points (cholera present state)

Here, we examine the presence of endemic equilibrium points which refers to the presence of stable solutions in the model where the cholera bacteria is persistently present in the population. These equilibrium points represent the stable disease states where the number of infected individuals and other compartments reaches a steady state. Mathematically, we find the endemic equilibrium points by setting the time derivatives of the model variables to zero and solving the resulting system of equations. These equilibrium points represent the stable solutions of the model where the disease persists over time, and they provide important clues about the long-term dynamics of the cholera disease in the population.

The endemic equilibrium points are defined as $(S_{H^*}(t), 0, S_{F^*}(t), 0)$ satisfying $S_H^*, I_H^*, R_H^*, S_{F,}^* I_H^* = 0$

Equating (3) and (4) to zero gives;

$$\begin{aligned} &\Gamma_H + \rho R_H - (\Psi_1+\mu_H)S_H = 0 \\ &\Psi_1 S_H - (\alpha+\mu_H+\delta)I_H = 0 \\ &\alpha I_H - (\rho+\mu_H)R_H = 0 \\ &\Gamma_F - (\Psi_2+\mu_F)S_F = 0 \\ &\Psi_2 S_F - \mu_F I_F = 0 \end{aligned} \tag{24}$$

Where

$$\Psi_1 = \frac{\beta_1 I_H}{1+\Phi I_H} + \frac{\beta_2 I_F}{1+\Phi I_F} \text{ and } \Psi_2 = \frac{\beta_3 I_F}{1+\Phi I_F}$$

Simplify the equation accordingly we have

$$R_H^* = \frac{(\Psi_1+\mu_H)(\alpha+\mu_H+\delta)(\rho+\mu_H) - \Gamma_H \alpha \Psi_1}{\rho \alpha \Psi_1}$$

$$S_H^* = \frac{(\alpha+\mu_H+\delta)(\rho+\mu_H)R_H^*}{\alpha \Psi_1}$$

$$I_H^* = \frac{(\rho+\mu_H)R_H^*}{\alpha} \tag{25}$$

$$S_F^* = \frac{\Gamma_F}{(\Psi_2+\mu_F)}$$

$$I_F^* = \frac{\Psi_2 \Gamma_F}{\mu_F(\Psi_2+\mu_F)}$$

From (25) it shows that the proposed population possesses a distinct endemic point which existed only when $R_0 < 1$.

3.7. Sensitivity analysis of the flies-human model

Here, we examine the sensitivity analysis of the flies-human bacteria model which involves studying how changes in the model's parameters affect the model's output or predictions. The goal is to understand which parameters have the most significant influence on the model's behavior and which ones have a lesser impact. This analysis helps in identifying the critical parameters that should be accurately.

So, the reproduction number analysis was performed $R_0 = \sqrt{R_{0H}R_{0F}}$ of the model which checks for the effect of a parameter on R_0 when increased or decreased.

Using the normalized Forward-Sensitivity Index of a variable R, on Y we obtain:

$$X_Y^R = \frac{\partial R}{\partial \beta} \cdot \frac{Y}{R} \tag{26}$$

The normalized sensitivity index of β1 obtained as:

$$X_{\beta_1}^{R_n} = \frac{\partial R_n}{\partial \beta_1} \cdot \frac{\beta_1}{R_n} \tag{27}$$

$$R_n = \sqrt{\frac{\beta_1 \beta_2 \beta_3 \Gamma_H \Gamma_F}{\mu_F^2 \mu_H (\alpha+\mu_H+\delta)(1+\Phi I_H)^2 (1+\Phi I_F)^2}}$$

Solving and computing the derivatives in (27) gives;

$$\frac{\partial R_n}{\partial \beta_1} = \frac{1}{2\beta_1} R_n. \text{ Then } X_{\beta_1}^{R_n} = \frac{\partial R_n}{\partial \beta_1} \cdot \frac{\beta_1}{R_n} = \frac{1}{2\beta_1} R_n \cdot \frac{\beta_1}{R_n}$$

$$X_{\beta_1}^{R_n} = +0.5$$

Thus we obtain the sensitivity index β1. In the same procedure, we evaluate the sensitivity indices for the parameters that made up of the reproduction number, the sensitivity indices of the parameters are given in the table below:

4. Interpretation of sensitivity indices

This analysis aids in determining which parameters have a significant impact on our investigation's findings. Nonetheless, some elements that are not very important in the real process of disease transmission are purposefully left out of the sensitivity analysis. For instance, parameters related to natural births and deaths in both humans and non-human primates are excluded because their impact on disease transmission is relatively minimal compared to other critical factors. Focusing on the most influential parameters allows us to gain greater understanding of the dynamics of the disease and better target control strategies for more effective disease management (see Table 1).

The estimated sensitivity indices for parameter R_n, are presented in Table 2. From the table, we observe that an increase in the values of parameters $\mu_H, \mu_F, \delta,$ and α leads to a decrease in the value of the parameter R_n. Conversely, a decrease in the values of parameters β_1, β_2, Γ_H, and Γ_F results in an increase in the number of cholera cases.

Table 1. The table includes human and flies state variables and parameter descriptions.

variables	Description
S_H	humans Susceptible
I_H	humans Infected
R_H	humans Recovered
S_F	Susceptible flies
I_F	Infected flies
Γ_H	Humans' recruitment rate
Γ_F	Flies' recruitment rate
β_1	Fies contact rate to humans
β_2	Human to humans contact rate
β_3	Flies to flies contact rate
μ_H	Humans' natural death rate
μ_F	Flies' natural death rate of flies
δ	The disease-induced rate for humans
ρ	Rate of being re-susceptible
ψ_1	Humans' rate of force of infection
ψ_2	Flies' rate of force of infection
α	humans Recovery rate

Table 2. Values of sensitivity indices for model parameters in Reproduction Number.

Parameters	Sensitivity indices (S.I)	Value of indices	Values	Sources
β_1	+	+0.5	0.04	Loyinmi et al., 2021
β_3	+	+0.5	0.005	Loyinmi et al., 2021
Γ_H	+	+0.5	1.2	Estimated
Γ_F	+	+0.5	0.70	Estimated
μ_H	−	−0.50311	0.0003465	Assumed
μ_F	−	−1	0.00261026	
δ_H	−	−0.0200378	0.01710615	
α	−	−0.4765122240	0.4	Assumed

This sensitivity analysis will help researchers to, identify key parameters, and assess robustness: optimize control strategies, and quantify uncertainty.

Overall, this sensitivity analysis provides valuable insights into the model's behavior and improves our understanding of the cholera disease dynamics in the flies-human system.

4.1. Optimal control strategies for cholera virus

The transmission rate is lowered by (1− *K*1), where *K*1 denote implementing efficient surveillance and early detection in affected regions to increase immunity in the population and reduce the risk of cholera outbreaks; k2 denote vaccination campaign and K3 connotes treatment: Implementing these three techniques to reduce the severity of outbreaks.

$$\left.\begin{aligned}\frac{dS_H}{dt} &= \Gamma_H + \rho R_H - (1-K_1)(\Psi_1+\mu_H)S_H\\ \frac{dI_H}{dt} &= (1-K_2)\Psi_1 S_H - (\alpha+\mu_H+\delta)k_3 I_H\\ \frac{dR_H}{dt} &= k_2 I_H - (\rho+\mu_H)R_H\end{aligned}\right\} \tag{28}$$

$$\left.\begin{aligned}\frac{dS_F}{dt} &= \Gamma_F - (\Psi_2+\mu_F)S_F\\ \frac{dI_H}{dt} &= \Psi_2 S_F - \mu_F I_F\end{aligned}\right\} \tag{29}$$

5. Analysis of the model incorporating preventive measures

Let $L=\{C_1,C_2,C_3\}\in L$ be Lebesgue measurable on $[0,1]$ where $0\le C(t)\le 1\in[0,1], i=1,2,3$

The objective function, O is given by

$$\mathrm{O}(K_1,K_2,K_3,) = \int_0^k \left(T_1R_H + T_2I_H + \frac{1}{2}\left(U_1K_1^2 + U_2K_2^2 + U_3K_3^2\right)\right)dt$$

Constraint to

$$\left.\begin{aligned}\frac{dS_H}{dt} &= \Gamma_H + \rho R_H - \Big((1-K_1)(\Psi_1+\mu_H)S_H\\ \frac{dI_H}{dt} &= (1-K_2)\Psi_1 S_H - (\alpha+\mu_H+\delta)k_3 I_H\\ \frac{dR_H}{dt} &= k_2 I_H - (\rho+\mu_H)R_H\end{aligned}\right\}$$

$$\left.\begin{aligned}\frac{dS_F}{dt} &= \Gamma_F - (\Psi_2+\mu_F)S_F\\ \frac{dI_H}{dt} &= \Psi_2 S_F - \mu_F I_F\end{aligned}\right\} \text{j}$$

The point of terminal is represented by the value *K*, where T_1, T_2 represent the weight constants attributed distinct group with the virus. Furthermore, our investigation extends to encompass an analysis of the social cost $U_1K_1^2$, $U_2K_2^2$ and $U_3K_3^2$. In order to establish the control problem, let

$$\begin{aligned}&(K_1{}^*(t),K_2{}^*(t)\,K_3{}^*(t)), \text{such that } O(K_1{}^*(t),k_2{}^*(t),\\ &\qquad K_3{}^*(t)) = \min\{O(K),(K)\in L\}\end{aligned} \tag{30}$$

6. Control analysis

We denote the control measures as k_1, k_2 and k_3. And assume δ is the infection probability, then the model equations become;

$$\begin{aligned}dS_H^1(t) &= \Gamma_H + eR_H - \frac{(1-k_1)\delta\beta_1 I_H S_H}{1+\varphi I_H} - \mu_H S_H\\ dI_H^1(t) &= \frac{(1-k_2)\delta\beta_1 I_H S_H}{1+\varphi I_H} - (\alpha+\mu_H+\delta)I_H\\ dR_H^1(t) &= \alpha I_H - (e+\mu_H)R_H + k_3 I_H\end{aligned} \tag{31}$$

7. Quantitative analysis of the model with control measures (t)

Using the maximum principle of Pontrgagin and creating an objective function, we present the presence of the control option in an analytical viable region [0, 1] signifying reduction in the transmission of the disease with $k=\{k_1,k_2,k_3\subset k\}$ measurable in

Lebesque terms [0, 1], $0 \le k_j \le 1 \subset [0,T]$, where $j = 1,2,3$.We present the objective function to be:

$$M(k_1,k_2,k_3) = \int \left[L_1 S + L_2 I + \frac{1}{2}\left(U_1 k_1^2 + U_2 k_2^2 + U_3 k_3^2\right)\right] dt \tag{32}$$

Equation (32) is constrained to (31) equipped with positive initial constrains, $S_H(0) > 0$, $I_H(0) > 0$ and $R_H(0) > 0$, U_1, U_2 and U_3 are fitted functions for the disease.

To establish the control problem, the function is implemented as;

$$M\left(k_1^*(t), k_2^*(t), k_3^*(t)\right) = \min\left\{M(k_1,k_2,k_3), k_1,k_2,k_3 \subset k\right\} \tag{33}$$

8. Presence of optimal measure (control)

Theorem 4. If we consider (33), setting k to be finite in (31) with initial constrains at $t \ge 0$, then $k^* = (k_1^*(t), k_2^*(t), k_3^*(t))$ exists in such a way that $M\{k_1^*(t), k_2^*(t), k_3^*(t)\} = \min\{M(k_1,k_2,k_3)\}, k_1,k_2,k_3 \subset k$

Proof

The integral of M to develop k_1, k_2, k_3, the positive region of the system pertaining to S_H, I_H, R_H, thus, the control to the model exists.

Next is to demonstrate the Hamiltonian (M) and Lagrangian (L) for the control problem. The Lagrangian is given by;

$$L = J_1 S + J_2 I + \frac{1}{2}\left(U_1 k_1^2 + U_2 k_2^2 + U_3 k_3^2\right) \tag{34}$$

And the Hamiltonian function is;

$$\begin{aligned} M = {} & J_1 S_H + J_2 I_H + \left(U_1 k_1^2 + U_2 k_2^2 + U_3 k_3^2\right) \\ & + \alpha_L S_H \left[\Gamma_H + eR_H - \frac{(1-k_1)\delta\beta_1 I_H S_H}{1+\varphi I_H} - \mu_H S_H\right] \\ & + \alpha_L I_H \left[\frac{(1-k_2)\delta\beta_1 I_H S_H}{1+\varphi I_H} - (\alpha + \mu_H + \delta) I_H\right] \\ & + \alpha_L R_H [\alpha I_H - (e+\mu_H) R_H + k_3 I_H] \end{aligned} \tag{35}$$

Where α_{L_i}, $i \in \{S_H, I_H, R_H\}$, by applying the constraints in theorem 5 to the Hamiltonian function and also differentiating (35) with respect to the state variables S_H, I_H, R_H, we obtain;

$$\begin{aligned} \frac{d\alpha_L S_H}{dt} &= J_1 + \alpha_L S_H \left[\frac{(1-k_1)\delta\beta_1 I_H}{1+\varphi I_H} - \mu_H\right] + \alpha_L I_H \left[\frac{(1-k_2)\alpha\beta_1 I_H}{1+\varphi I_H}\right] \\ \frac{d\alpha_L I_H}{dt} &= J_2 + \alpha_L S_H \left[\frac{(1-k_1)\delta\beta_1 S_H}{(1+\varphi I_H)^2}\right] + \alpha_L I_H \left[\frac{(1-k_2)\delta\beta_1 S_H}{(1+\varphi I_H)^2} - (\alpha+\mu_H+\delta) I_H\right] \\ & + \alpha_L R_H(\alpha) \\ \frac{d\alpha_L R_H}{dt} &= \alpha_L S_H (e) + \alpha_L R_H (e + \mu_H) \end{aligned} \tag{36}$$

Differentiating (36) and considering (35) with respect to the control parameters k_1, k_2 and k_3, we obtain;

$$\frac{dk_1}{dt} = U_1 k_1 - \alpha_L S_H \frac{\delta\beta_1 I_H S_H}{1+\varphi I_H} = 0 \Rightarrow k_1 = \alpha_L S_H \frac{\delta\beta_1 I_H S_H}{U_1(1+\varphi I_H)} \tag{37}$$

$$\frac{dk_2}{dt} = U_2 k_2 - \alpha_L I_H \frac{\delta\beta_1 I_H S_H}{1+\varphi I_H} = 0 \Rightarrow k_2 = \alpha_L I_H \frac{\delta\beta_1 I_H S_H}{U_2(1+\varphi I_H)} \tag{38}$$

$$\frac{dk_3}{dt} = U_3 k_3 - \alpha_L R_H I_H \;\Rightarrow\; k_3 = \frac{\alpha_L R_H I_H}{U_3} \tag{39}$$

Applying the condition of transversality, we obtain;

$$k_1^* = \min\{1, \max\{0, c_1\}\}, k_2^* = \min\{1, \max\{0, c_2\}\},$$
$$k_3^* = \min\{1, \max\{0, c_3\}\} \text{ where } c_1 = \alpha_L S_H \frac{\delta\beta_1 I_H S_H}{U_1(1+\varphi I_H)},$$
$$c_1 = \alpha_L I_H \frac{\delta\beta_1 I_H S_H}{U_2(1+\varphi I_H)} \text{ and } c_3 = \frac{\alpha_L R_H I_H}{U_3}$$

This completes the proof.

8.1. Numerical solution

We approach the sets of differential equations used numerically by using one of the well-known method called Finite Difference Scheme (FSD) in order to achieve numerical values (see Fig. 2).

$$\left.\begin{aligned} \frac{dS_H}{dt} &= \Gamma_H + \rho R_H - (\psi_1 + \mu_H) S_H \\ \frac{dI_H}{dt} &= \psi_1 S_H - (\alpha + \mu_H + \delta) I_H \\ \frac{dR_H}{dt} &= \alpha I_H - (\rho + \mu_H) R_H \\ \frac{dS_F}{dt} &= \Gamma_F - (\psi_2 + \mu_F) S_F \\ \frac{dI_F}{dt} &= \psi_2 S_F - \mu_F I_F \end{aligned}\right\} \tag{40}$$

$$S_H(t) \ge 0, I_H(t) \ge 0, R_H(t) \ge 0, S_F(t) \ge 0, I_F(t) \ge 0,$$

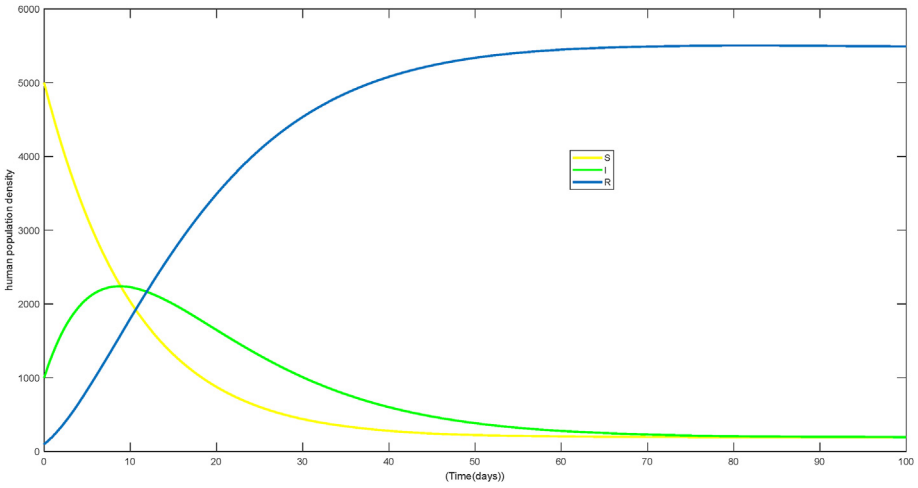

Fig. 2. Solution trajectories of human population without control.

Using the finite difference as stated earlier (40) can be decomposed as;

$$\frac{S_{H(J+1)} - S_{HJ}}{h} = \Gamma_H + \rho R_{HK} - (\psi_1 + \mu_H) S_{HK}$$

$$\frac{I_{H(J+1)} - I_{HJ}}{h} = \psi_1 S_{HK} - (\alpha + \mu_H + \delta) I_{HK}$$

$$\frac{R_{H(J+1)} - R_{HJ}}{h} = \alpha I_{HK} - (\rho + \mu_H) R_{HK} \quad (41)$$

$$\frac{S_{F(J+1)} - S_{FJ}}{h} = \Gamma_F - (\psi_2 + \mu_F) S_{FK}$$

$$\frac{I_{F(J+1)} - I_{FJ}}{h} = \psi_2 S_{FK} - \mu_F I_{FK}$$

(41) Can be alternatively be written as;

$$S_{H(J+1)} = S_{HJ} + h(\Gamma_H + \rho R_{HK} - (\psi_1 + \mu_H) S_{HK})$$

$$I_{H(J+1)} = I_{HJ} + h(\psi_1 S_{HK} - (\alpha + \mu_H + \delta) I_{HK})$$

$$R_{H(J+1)} = R_{HJ} + h(\alpha I_{HK} - (\rho + \mu_H) R_{HK}) \quad (42)$$

$$S_{F(J+1)} = S_{FJ} + h(\Gamma_F - (\psi_2 + \mu_F) S_{FK})$$

$$I_{F(J+1)} = I_{FJ} + h(\psi_2 S_{FK} - \mu_F I_{FK})$$

Where $J = 0, 1, 2, 3, 4, 5\ldots$, h is step size

8.2. Numerical simulation

In this section, we deploy a means to observe the propagation of the disease with respect time, track constraints in various parameters, and evaluate the effectiveness of control plan. The state variables' initial conditions are as follows:,

$S_H = 5000$, $I_H = 1000$, $R_H = 100$, $S_F = 1000$ and $I_F = 500$. Also, $\psi_1 = 0.091193$; $\psi_2 = 0.32$ and the parameter values needed for the simulation are displayed in Table 2

9. Discussion

In Fig. 3 The increase in the human susceptible class indicate the effect of the combined control measures in this category of population. This is a positive outcome as it means that a larger portion of

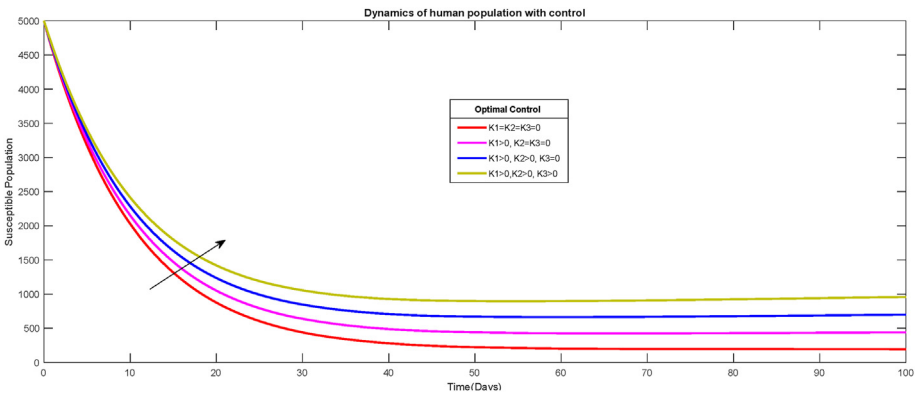

Fig. 3. Solution trajectories of susceptible population with (out) optimal control.

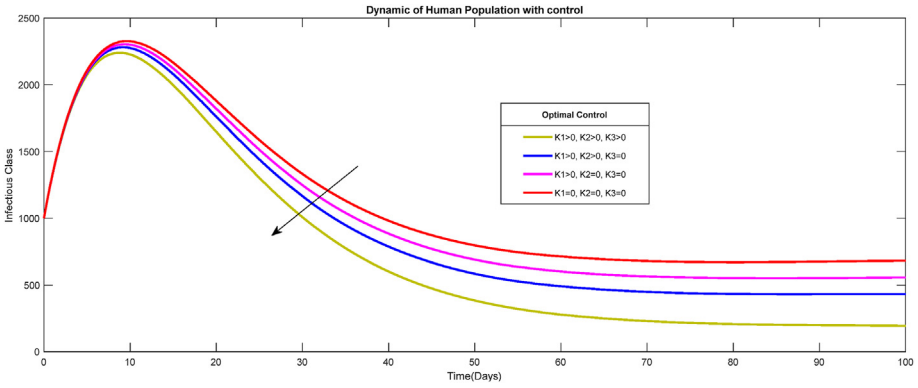

Fig. 4. Solution trajectories of susceptible population with (out) optimal control.

the population is gaining immunity against cholera. By increasing immunity, the risk of cholera outbreaks is reduced. The susceptible individuals who become immune via the cumulative effect of these controls are no longer at risk of contracting cholera, leading to a decline in the number of cases. Also the increase in the human susceptible class also suggest that early detection, vaccination measures and successfully identifying and treating cholera cases. When cholera cases are promptly identified and treated, the infected individuals are less likely to contribute to the spread of the disease, as they are no longer in the susceptible category. Efficient surveillance, Vaccination campaign and treatment can break the chain of transmission and limit the severity of cholera outbreaks. In summary, the increase in the human susceptible class in Fig. 3 indicates that the three optimal control measures, vaccination campaigns efficient surveillance and treatment, are effectively reducing the susceptibility of the population to cholera. This, in turn, leads to a positive impact on cholera control by decreasing the likelihood of outbreaks and reducing the severity of the disease when cases do occur.

Fig. 4 shows that the decrease in the human infected class indicates that the implementation of these three optimal control measures is effective in reducing the number of people infected with cholera. This is a positive outcome, as it signifies a lower disease burden in the population. The decline in the human infected class suggests that these control measures are successful in curbing the transmission of cholera within the population. Efficient surveillance and vaccination campaigns help increase immunity, while early treatment prevent the disease from spreading rapidly. The decrease in the number of infected individuals has a positive impact on public health. It means fewer people are getting sick, leading to lower morbidity and, hopefully, a decrease in cholera-related mortality. The effectiveness of these control measures in reducing the human infected class underscores the importance of timely and proactive intervention strategies. Early detection and treatment are critical in preventing severe outbreaks. In summary, Fig. 4 shows that implementing these three control measures have a positive impact on reducing cholera infections in the population. These control measures are effective in decreasing the spread of the disease and improving public health outcomes by reducing the burden of cholera.

In Fig. 5, in the human recovered class (recovery from cholera) increases from (0–10 days). This

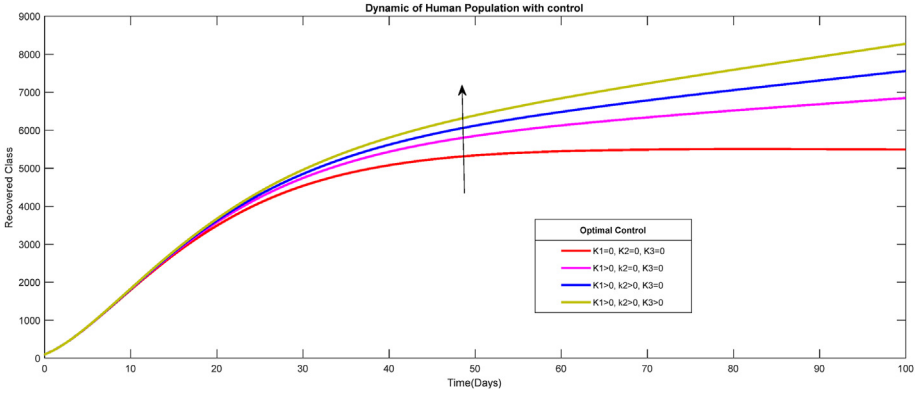

Fig. 5. Solution trajectories of population with (out) optimal control.

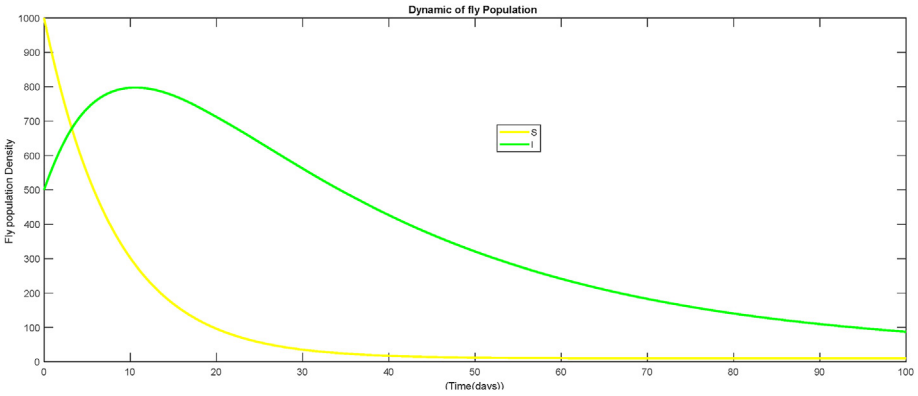

Fig. 6. Solution trajectories of fly population without saturation.

suggests that the efficient surveillance and vaccination campaigns are effectively increasing immunity in the population, which results in a higher number of individuals recovering from cholera more quickly. The positive impact of this control measure is that it helps to reduce the number of people who become infected with cholera and, as a result, the duration of illness. This ultimately leads to a decrease in the number of people suffering from cholera and its associated complications. The human recovered class increases from 0 to 10 days, indicating that early detection, vaccination and prompt treatment are effective in reducing the duration of cholera in infected individuals, the positive impact of this control measure is that it helps identify cholera cases early, enabling timely treatment, which is crucial for reducing the severity of the disease and preventing further transmission. Overall, based on Fig. 5, it appears that these control measures have a positive impact on reducing the severity and duration of cholera cases in the population up to a certain point (10 days) and beyond, the impact of the surveillance and treatment measure may decrease, but it's still essential for managing the outbreak effectively. These control measures are crucial in mitigating the impact of cholera and preventing its rapid spread (see Fig. 6).

In Fig. 7. Saturation was introduced in fly population as a form of control which could be in form pesticide and any other form to combat fly population which acts as the carrier, as this factor decrease the flies' infected class and increase the susceptible class. This can be considered a positive outcome, meanwhile, it indicates that the control measures are primarily affecting the human population, which is the intended target. You don't want the fly population to increase as it can act as a vector for cholera transmission. These control measures are designed to reduce the human-to-human transmission of cholera and enhance early detection and treatment. If the fly population were affected, it might imply unintended consequences or ecological disruptions. The key goal of these control measures is to reduce the severity of cholera outbreaks in the human population, by increasing immunity through proposed control techniques, these measures can effectively reduce the number of cholera cases and associated human suffering.

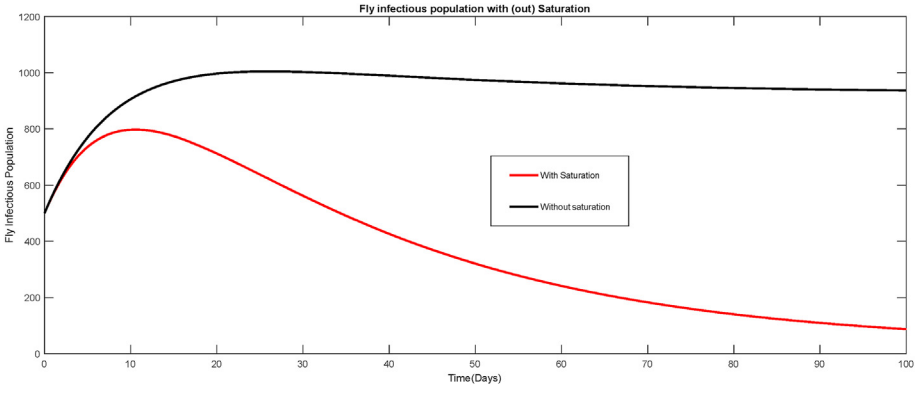

Fig. 7. Solution trajectories of fly population with (out) saturation.

10. Conclusion

In conclusion, the findings presented in this research paper underscore the effectiveness of three critical control measures in the battle against cholera: effective surveillance, vaccination campaigns and treatment. The various figures and analyses throughout the study reveal the positive impact of these interventions on reducing the susceptibility, infection rate, severity, and duration of cholera cases within the human population. Fig. 3 demonstrated that an increase in the human susceptible class signifies a greater portion of the population gaining immunity against cholera through vaccination and efficient surveillance. This not only reduces the risk of cholera outbreaks but also limits the severity of the disease when cases do occur. Treatment break the chain of transmission, further minimizing the impact of outbreaks. Fig. 4 illustrated a decrease in the human infected class, indicating the successful reduction of cholera cases through these control measures. This outcome is significant, as it implies a lower disease burden, lower morbidity, and, ultimately, a decrease in cholera-related mortality. Fig. 5 provided insights into the rapid recovery of individuals from cholera, up to a certain point (10 days), thanks to vaccination campaigns, early detection and treatment. The timely identification of cholera cases and treatment remains crucial for reducing the severity of the disease, even as recovery rates might decrease after a specific time frame. Fig. 7 demonstrated that these control measures do not significantly impact the fly population, thus preserving ecological stability. However saturation factor works as a form of control in fly population which reduces infected class, as it indicates that the control measures effectively target human-to-human transmission routes without unintended ecological consequences.

Overall, this research paper's findings highlight the crucial role of vaccination campaigns, efficient surveillance and treatment in controlling cholera. These measures contribute to the reduction of susceptibility, infection, severity, and duration of cholera cases in the human population, ultimately leading to improved public health outcomes. By minimizing the impact of outbreaks and preventing rapid disease transmission, these interventions offer hope in the ongoing fight against cholera, showcasing their value in safeguarding the well-being of affected communities.

11. Future work and limitations

In order to localize response, we do aim to expand the study to small geographical scale spatial modeling of the disease in the future. However, obtaining precise and reliable data is a hurdle in developing a model that is based on real data. This allows us to concentrate on creating predictive models that can estimate the possible course of the epidemic, allowing for the early deployment of resources and measures to inhibit the disease's spread.

Data availability

No datasets generated during and/or analyzed during the current study.

Acknowledgement

Mrs Adetoun Loyinmi is appreciated for her support.

References

[1] Hethcote HW. The mathematics of infectious diseases. SIAM Rev 2000;42(4):599–653.
[2] Loyinmi AC, Gbodogbe SO. Mathematical modeling and control strategies for Nipah virus transmission incorporating Bat – to – pig –to – human pathway. EDUCATUM J Sci, Math Technol 2024;11(1):54–80. https://doi.org/10.37134/ejsmt.vol11.1.7.2024.
[3] Loyinmi AC, Gbodogbe SO, Idowu KO. On the interaction of the human immune system with foreign body: mathematical modeling approach. Kathmandu Univ J Sci Eng Technol 2023;17(2):1–17. https://journals.ku.edu.np/kuset/article/view/137.
[4] World Health Organization. Prevention and control of cholera outbreaks: WHO policy and recommendations. WHO position paper on prevention and control of cholera outbreak, vol. 1; 2009. p. 12. http://www.who.int/cholera/technical/prevention/control/en/index.html.
[5] Loyinmi AC, Idowu KO. Semi –analytical approach to solving Rosenau-Hyman and Korteweg-de Vries equations using integral transform. Tanzan J Sci 2023;49:26–40. https://doi.org/10.4314/tjs.v49il.3.
[6] Agbomola J, Loyinmi A. A mathematical model for the dynamical behavior of Ebola in human-bat population: implication of immediate discharge of recovered individuals. Preprints 2022. https://doi.org/10.21203/rs.3.rs-1399224/v1.
[7] Loyinmi AC, Lawal OW, Sottin DO. Reduced differential transform method for solving partial integro-differential equation. J Niger Assoc Math Phys 2017;43:37–42.
[8] Loyinmi AC, Oredein AI, Prince SU. Homotopy adomian decomposition method for solving linear and nonlinear partial differential equations. Tasued J Pure Appl Sci 2018;1:254–60.
[9] Nelson EJ, Harris JB, Morris JG, Calderwood SB, Camilli A. Cholera transmission: the host, pathogen and bacteriophage dynamic. Nat Rev Microbiol 2009;7(10):693–702.
[10] Loyinmi AC, Akinfe TK, Ojo AA. Qualitative analysis and dynamical behavior of a Lassa haemorrhagic fever model with exposed rodents and saturated incidence rate. Scientific African 2021;14:e01028. https://doi.org/10.1016/j.sciaf.2021.e01028.
[11] Loyinmi AC, Oredein AI. The unsteady variable viscosity free convection flow on a porous plate. J Niger Assoc Math Phys 2011;19:229–32. https://www.ajol.info/index.php/jonamp/article/view/91459.
[12] World Health Organization Media centre, Cholera factsheet N107. [Accessed on 23 August 2018]. Available at: http://www.who.int/mediaBcentre/factsheets/fs107/en/b.
[13] Ryan ET. The cholera pandemic, still with us after half a century: time to rethink, PLOS Neglect. Trop Diseases 2011;5(1):e1003.

[14] Loyinmi AC, Erinle-Ibrahim LM, Adeyemi AE. The new iterative method (NIM) for solving telegraphic equation. J Niger Assoc Math Phys 2017;43:31−6.
[15] Lawal OW, Loyinmi AC, Arubi DA. Approximate solutions of higher dimensional linear and nonlinear initial boundary problems using new iterative method. J Niger Assoc Math Phys 2017;41:35−40.
[16] World health organization (WHO). web page, www.who.org; 2015.
[17] Lawal OW, Loyinmi AC. The effect of magnetic field on MHD viscoelastic flow and heat transfer over a stretching sheet. Pioneer J Adv Appl Math 2011;3:83−90.
[18] Loyinmi AC, Ijaola AL. Fractional order model of dynamical behavior and qualitative analysis of Anthrax with infected vector and saturation. Preprints 2024. https://doi.org/10.20944/preprints202403.0632.v1.
[19] Kermack WO, McKendrick AG. A contribution to the mathematical theory of epidemics. Proc R Soc Lond - Ser A Contain Pap a Math Phys Character 1927;115(772):700−21.
[20] Capass V, Paveri-Fontana SL. A mathematical model for the 1973 cholera epidemic in the European Mediterranean region. Revue d'épidémiologie et de Santé Publique 1979;27(2):121−32.
[21] Erinle-Ibrahim LM, Adewole AI, Loyinmi AC, Sodeinde OK. An optimization scheme using linear programming in a production line of rites food limited, Ososa. FUDMA J Sci 2020;4:502−10.
[22] Idowu OK, Loyinmi AC. Qualitative analysis of the transmission dynamics and optimal control of covid-19. EDUCATUM J Sci, Math Technol 2023;10(1):54−70. https://doi.org/10.37134/ejsmt.vol10.1.7.2023.
[23] Lipp EK, Huq A, Colwell RR. Effects of global climate on infectious disease: the cholera model. Clin Microbiol Rev 2002;15(4):757−70.
[24] Lawal OW, Loyinmi AC, Sowumi SO. Homotopy perturbation algorithm using Laplace transform for linear and nonlinear ordinary delayed differential equation. J Niger Assoc Math Phys 2017;41:27−34.
[25] Lawal OW, Loyinmi AC. Application of new iterative method for solving linear and nonlinear initial boundary value problems with non-local conditions. Sci World J 2019;14:100−4.
[26] Jensen MA, Faruque SM, Mekalanos JJ, Levin BR. Modeling the role of bacteriophage in the control of cholera outbreaks. Proc Natl Acad Sci USA 2006;103(12):4652−7.
[27] Lawal OW, Loyinmi AC, Hassan AR. Finite difference solution for Magneto hydrodynamics thin film flow of a third grade fluid down inclined plane with ohmic heating. J Math Assoc Niger 2019;46:92−7.
[28] Lawal OW, Loyinmi AC. Magnetic and porosity effect on MHD flow of a dusty visco-elastic fluid through horizontal plates with heat transfer. J Niger Assoc Math Phys 2012;21:95−104.
[29] Idowu KO, Loyinmi AC. Impact of contaminated surfaces on the transmission dynamics of corona virus disease (Covid-19). Biomed J Sci Tech Res 2023;51:42280−90. https://doi.org/10.26717/BJSTR.2023.51.008046.
[30] Idowu KO, Loyinmi AC. The analytical solution of non-linear Burgers- Huxley equations using the Tanh method. Al-Bahir J Eng Pure Sci 2023;3:68−77. https://doi.org/10.55810/2312-5721.1038.
[31] Longini Jr IM, Nizam A, Ali M, Yunus M, Shenvi N, Clemens JD. Controlling endemic cholera with oral vaccines. PLoS Med 2007;4(11):e336.
[32] Lawal OW, Loyinmi AC, Erinle-Ibrahim LM. Algorithm for solving a generalized Hirota-Satsuma coupled KDV equation using homotopy perturbation transformed method. Sci World J 2018;13:23−8.
[33] Agbomola JO, Loyinmi AC. Modelling the impact of some control strategies on the transmission dynamics of Ebola virus in human-bat population: an optimal control analysis. Heliyon, 8:e12121. https://doi.org/10.1016/j.heliyon.2022.e12121.
[34] Neilan RLM, Schaefer E, Gaff H, Fister KR, Lenhart S. Modeling optimal intervention strategies for cholera. Bull Math Biol 2010;72(8):2004−18.
[35] Lawal OW, Loyinmi AC, Ayeni OB. Laplace homotopy perturbation method for solving coupled system of linear and nonlinear partial differential equation. J Math Assoc Niger 2019;46:83−91.
[36] Lot S, Lawal OW, Loyinmi AC. Magnetic field's effect on two phase flow of Jeffery and non- Jeffery fluid with partial slip and heat transfer in an inclined medium. Al − Bahir J Eng Pure Sci 2024;4(1):71−9. https://doi.org/10.55810/2313-0083.1054.
[37] Loyinmi AC, Akinfe TK. An algorithm for solving the Burgers-Huxley equation using the Elzaki transform. SN Appl Sci 2020;2:1−17. https://doi.org/10.1007/s42452-019-1652-3.
[38] Mwasa A, Tchuenche JM. Mathematical analysis of a cholera model with public health interventions. Biosystems 2011;105(3):190−200.
[39] Loyinmi AC, Akinfe TK. Exact solution to the family of Fisher's reaction-diffusion equations using Elzaki homotopy transformation perturbation method. Eng Reports 2020;2:e12084. https://doi.org/10.1002/eng2.12084.
[40] Idowu KO, Akinwande TG, Fayemi I, Adam UM, Loyinmi AC. Laplace homotopy perturbation method (LHPM) for solving system of N-dimensional non-linear partial differential equation. Al-Bahir J Eng Pure Sci 2023;3:11−27. https://doi.org/10.55810/2312-5721.1031.
[41] Loyinmi AC, Lawal OW. The asymptotic solution for the steady variable-viscosity free convection flow on a porous plate. J Niger Assoc Math Phys 2011;19:273−6.
[42] Lawal OW, Loyinmi OW. Oscillating flow on a visco-elastic fluid under exponential pressure gradient with heat transfer. Pioneer J Adv Appl Math 2011;3:33−82.
[43] Lemos-Paião AP, Silva CJ, Torres DF. An epidemic model for cholera with optimal control treatment. J Comput Appl Math 2017;318:168−80.
[44] Loyinmi AC. Analysis of two hybrid schemes to solve the Benjamin-Bona-Mahony (BBM) equation. Kathmandu Univ J Sci Eng Technol 2024;18:1−15. https://doi.org/10.3126/kuset.v18i1.67498.